FOURIER-HERMITE COMMUNICATIONS; WHERE FOURIER MEETS HERMITE

C. Willem Korevaar, André B.J. Kokkeler, Pieter-Tjerk de Boer, Gerard J.M. Smit

Department of Electrical Engineering, Mathematics and Computer Science
University of Twente, The Netherlands
Email: c.w.korevaar@utwente.nl

ABSTRACT

A new signal set, based on the Fourier and Hermite signal bases, is introduced. It combines properties of the Fourier basis signals with the perfect time-frequency localization of the Hermite functions. The signal set is characterized by both a high spectral efficiency and good time-frequency localization. Its robustness against time-frequency shifts is assessed and compared to Hermite and Fourier basis signals. The Fourier-Hermite signal set is particularly designed for communications in spectrum-scarce environments.

Index Terms— Fourier-Hermite signals, multi-carrier communications, time-frequency analysis

1. INTRODUCTION

The Fourier basis - consisting of complex exponentials of different frequency - is the dominant signal basis in communication systems nowadays. Orthogonal frequency division multiplexing (OFDM) is a multi-carrier scheme based on the modulation of time-limited Fourier-basis signals and is applied in many communication standards. Despite its popularity, OFDM is also associated with some drawbacks like spectral leakage and a high sensitivity for frequency offsets [1]. To reduce these problems, it is common to filter the OFDM signal prior to transmission. However, instead of modifying the transmit signal, the signal basis itself can be reconsidered. Especially given the scarcity of spectrum and the rise of cognitive radios, the quest is on for spectrally efficient, time-frequency localized signal bases for communication systems.

Hermite functions form a set of orthogonal signals, are maximally localized in time and frequency (according to their second order moments over time and frequency [2]), are eigenfunctions of the fractional Fourier transform (FrFT) [3] and are the eigenfunctions of wide-sense stationary uncorrelated scattering (WSSUS) doubly dispersive channels characterized by an elliptical scattering function [4, 5]. Summing up, Hermite functions are an interesting candidate as a signal basis for wireless communication systems. However, they also offer some key challenges. One of these challenges is the sensitivity of higher order Hermite functions for a time and/or frequency offset. This is caused by a sharp concentration of the ambiguity function (AF) [5] and is similar to the sensitivity of some wavelets to time or frequency offsets [6].

Section 2 introduces the Fourier-Hermite signal set, which is the main contribution of this paper. The proposed signal set attains both a high spectral efficiency and is well localized in time-frequency. Its spectral efficiency and robustness against time- and frequency offsets is treated in Section 3. Sections 4 and 5 include a qualitative comparison with prior work and conclude this paper.

2. THE FOURIER-HERMITE SIGNAL SET

We describe a continuous, baseband multi-carrier signal as the sum of K different subcarrier signals $s_k(t)$,

$$x(t) \triangleq \sum_{k=0}^{K-1} A_k s_k(t), \tag{1}$$

where A_k represents a (complex) value corresponding to the modulation scheme chosen. In additive white Gaussian noise (AWGN) channels, orthogonality among the subcarriers $s_{k'}$ and $s_{k \neq k'}$ is a requirement to recover the information A_k at the receiver without noise amplification. In addition to orthogonality, spectral efficiency, spectral leakage, the peak-to-average power ratio (PAPR), robustness against fading and for time- and frequency-offsets are of importance as well.

2.1. A Fourier based signal set

The dominant signal set in time-invariant signal analysis and communications is based on complex exponentials,

$$s_{k,\mathrm{F}}(t) \triangleq e^{j2\pi k \frac{t}{T_s}} \qquad t \in [-T_s/2, T_s/2], \tag{2}$$

where j is the imaginary unit. The symbol time T_s can be chosen in correspondence with the channel conditions; e.g. based on the duration of the channel impulse response. The Wigner distribution function (WDF) is used to provide a two-dimensional joint time-frequency distribution $W(t, \omega)$ of the signal $s_k(t)$ [7, 8]:

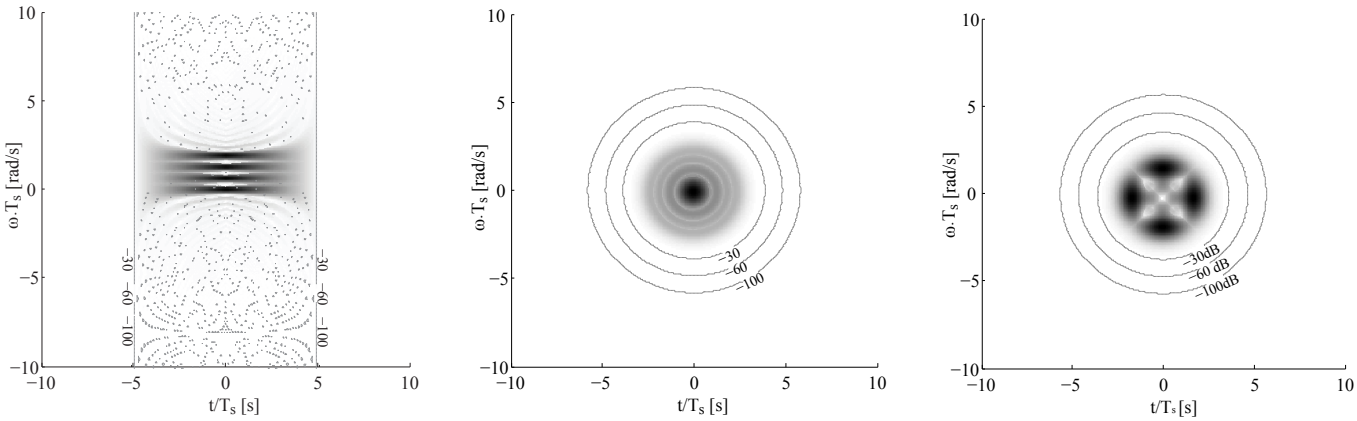

(a) (b) (c)

Fig. 1. Illustration of the time-frequency distribution - by means of the Wigner distribution function (WDF) [7] - of four lowest order signals of the (a) Fourier basis (b) Hermite basis and (c) Fourier-Hermite signal set. The gray lines indicate the -30dB, -60dB and -100dB levels of the WDF. The noisy pattern in (a) shows the -30dB contours of some sidelobes.

$$W(t,\omega) \triangleq \frac{1}{2\pi}\int_{-\infty}^{\infty} s_k\left(t+\frac{t'}{2}\right)\overline{s_k\left(t-\frac{t'}{2}\right)}e^{-j\omega t'}\,dt'\,. \tag{3}$$

The strict time-limitedness of the signals $s_{k,\mathrm{F}}(t)$ leads to poor localization in frequency as shown by the WDF in Fig. 1a.

2.2. A Hermite based signal set

Hermite functions are characterized by oscillations both in time and frequency. An orthonormal signal set consisting of Hermite functions $s_{k,\mathrm{H}}(t)$ is defined by [4];

$$s_{k,\mathrm{H}}(t) \triangleq h_k\left(\frac{t}{T_s}\right) = \frac{1}{\sqrt{2^k k!\sqrt{\pi}\cdot T_s}}\cdot H_k\left(\frac{t}{T_s}\right)\cdot e^{-\frac{t^2}{2T_s^2}}$$
$$\text{with } H_k(t) = (-1)^k\, e^{t^2}\frac{d^k}{dt^k}\left(e^{-t^2}\right). \tag{4}$$

As stated in Section 1, a Hermite function $h_k(t)$ of order k is an eigenfunction of the unitary (fractional) Fourier transform with eigenvalue λ_k [3];

$$\mathcal{F}^{\alpha}\left\{h_k(t)\right\}(u) \triangleq \int_{-\infty}^{\infty} K_\alpha(t,u)h_k(t)dt = \lambda_k h_k(u), \tag{5}$$

where $\mathcal{K}_\alpha$ is the kernel of the FrFT;

$$K_\alpha(t,u) \triangleq \begin{cases} \sqrt{\frac{1-j\cot(\alpha)}{2\pi}}\cdot e^{j\frac{u^2+t^2}{2}\cot(\alpha)}\cdot e^{-jut\csc(\alpha)} & \\ \delta(t-u) & \text{if } \alpha = p\cdot 2\pi,\ p\in\mathbb{Z} \\ \delta(t+u) & \text{if } \alpha = \pi + p\cdot 2\pi,\ p\in\mathbb{Z}\,. \end{cases}$$

The FrFT rotates the signal presentation in time-frequency over an angle α with the time-axis and is periodic with 2π. The WDFs of four lowest order Hermite functions are shown in Fig. 1b. The -30dB and -60dB levels of the WDF show that Hermite functions have their energy localized in a relatively small time-bandwidth area compared to Fourier basis signals.

2.3. The Fourier-Hermite signal set

The perfect time-frequency localization as well as the discussed eigenfunction properties of Hermite functions justify our interest in this signal set for communications. However, a primary challenge is the order-dependent signal-behavior of Hermite functions. Lower order Hermite functions - like the zeroth order Gaussian signal - are known to be robust against a time-frequency offset. This is in contrast to higher order Hermite functions, which become increasingly sensitive to a time-frequency offset. The approach taken is to average the properties of different Hermite functions by constructing a new signal set where each signal is a weighted sum of Hermite functions. By applying an orthogonal transform to orthonormal Hermite functions, a new orthogonal signal set is obtained. The inverse discrete Fourier transform (DFT) is used because of the cyclic properties of the Fourier basis, but other orthogonal transforms may prove useful as well. We now define a set of K Fourier-Hermite signals $s_{k,\mathrm{FH}}(t)$ as,

$$s_{k,\mathrm{FH}}(t) \triangleq \frac{1}{K}\sum_{n=0}^{K-1} e^{j2\pi\frac{k\cdot n}{K}}h_n(t), \tag{6}$$

which can be written in matrix-form. E.g., if $K=4$ we get

$$\begin{bmatrix} s_{0,\mathrm{FH}}(t) \\ s_{1,\mathrm{FH}}(t) \\ s_{2,\mathrm{FH}}(t) \\ s_{3,\mathrm{FH}}(t) \end{bmatrix} = \frac{1}{4}\cdot\begin{bmatrix} 1 & 1 & 1 & 1 \\ 1 & j & -1 & -j \\ 1 & -1 & 1 & -1 \\ 1 & -j & -1 & j \end{bmatrix}\cdot\begin{bmatrix} h_0(t) \\ h_1(t) \\ h_2(t) \\ h_3(t) \end{bmatrix}. \tag{7}$$

The signals $s_{k,\mathrm{FH}}$ are mutually orthogonal and their time-frequency distribution is shown in Fig. 1c for $K=4$ and in Fig. 3 for $K=32$. The 'sidelobes' of the Fourier-Hermite pulses are in-band in contrast to conventional OFDM signals

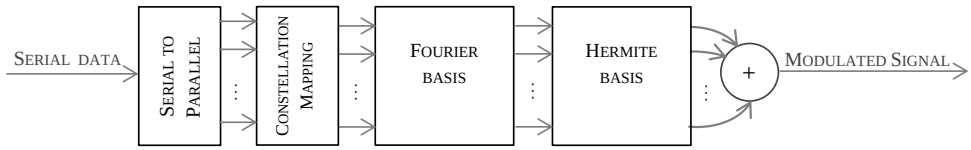

Fig. 2. Overview of the generation of a baseband transmit signal by modulation of Fourier-Hermite signals.

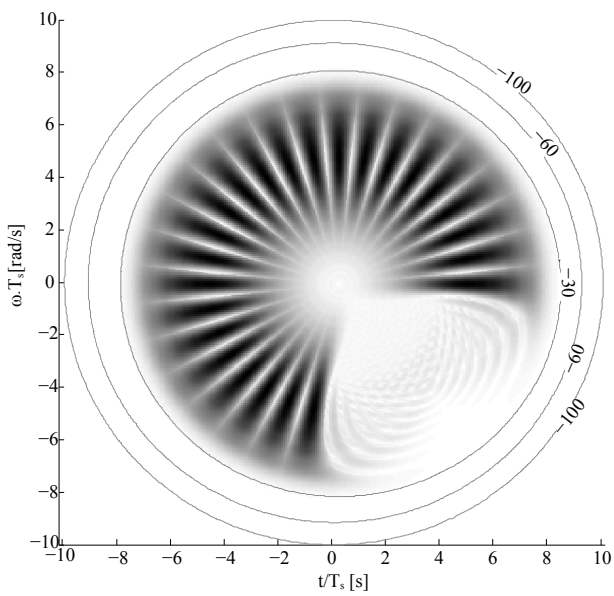

Fig. 3. The Wigner distribution function (WDF) of 24 Fourier-Hermite signals out of a set of 32 ($K = 32$) exhibits in-band 'sidelobes'. The gray lines indicate the -30dB, -60dB and -100dB levels of the WDF.

where part of the sidelobes are out-of-band. Note that an equivalent description of the signals $s_{k,\mathrm{FH}}(t)$ is obtained by time-frequency rotated versions of $s_{0,\mathrm{FH}}(t)$, i.e.;

$$s_{k,\mathrm{FH}}(t) = \mathcal{F}^{\frac{2\pi k}{K}}\left(\sum_{n=0}^{K-1} h_n(t)\right) \text{ for } k = 0 \ldots K-1. \quad (8)$$

Concluding, a Fourier-Hermite signal set with K signals consists of one signal which is the sum of K Hermite functions and there are $K-1$ time-frequency rotated versions. An illustration of the generation and modulation of Fourier-Hermite signals is provided in Fig. 2.

3. PERFORMANCE ASSESSMENT

3.1. Spectral efficiency

The Fourier-Hermite signal set has a time-bandwidth product proportional to the number of Hermite functions used in the set [2]. Hermite and Fourier-Hermite functions are neither strictly time-limited nor strictly band-limited. Although dependent on the exact time-duration and bandwidth definitions used, Fig. 3 reveals that a set of 32 Fourier-Hermite signals has the larger amount of energy contained in time-frequency area with a radius of 8. The time-bandwidth product for these 32 signals is approximately $\pi \cdot 8^2 / (2 \cdot \pi) = 32$. Given quadrature modulation, Fourier-Hermite signals, similar to OFDM, allow for roughly 2 degrees of freedom per unit time-bandwidth. However, efficiently filling up the time-frequency plane by Fourier-Hermite signal sets is more problematic due to the circular shape of the time-frequency distribution. In contrast, the Fourier basis signals and in particular orthogonal frequency division multiple access (OFDMA) enable multiple spectrum users to communicate with maximum spectral efficiency, under the assumption of perfect timing and frequency synchronization among spectrum users.

In practice, perfect timing and frequency synchronization is often not supported by the users or hard to attain. When multiple users are not perfectly synchronized, it is of importance to limit mutual interference among users. As can be deducted from Fig. 1a-1c, the time-frequency localization of (Fourier-)Hermite functions is considerably better than for conventional Fourier-based signals. Therefore, when spectrum users are unsynchronized, a communication system employing Fourier-Hermite signals could be beneficial over Fourier basis signals.

3.2. Robustness against a time-frequency offset

The (narrowband) ambiguity function (AF) $\mathcal{A}_{f,g}(\nu,\tau)$ of two functions $f(t)$ and $g(t)$ evaluates the matched filter output in case of a time-frequency shifted signal [7, 8].

$$\mathcal{A}_{f,g}(\nu,\tau) \triangleq \int_{-\infty}^{\infty} f\left(t+\frac{\tau}{2}\right) \cdot \overline{g\left(t-\frac{\tau}{2}\right)} e^{j\nu t} dt\,. \quad (9)$$

The AF is used to calculate the inter-carrier interference for a signal set which is affected by a time-frequency shift due to, for example, time offsets or Doppler shifts. We have performed simulations using signal sets based on Fourier signals $s_{k,\mathrm{F}}$, Hermite functions $s_{k,\mathrm{H}}$ and Fourier-Hermite signals $s_{k,\mathrm{FH}}$. The signals are modulated by QPSK. With $K = 4$ the auto-ambiguity function for $s_{0,\mathrm{FH}}$ is shown in Fig. 4. Based on M symbols with $M = 500$, the average signal-to-interference ratio (SIR) has been calculated as a function of ν and τ;

$$\overline{\mathrm{SIR}}(\nu,\tau) \triangleq \frac{1}{K}\sum_{k=0}^{K-1} \frac{\frac{1}{M}\sum_{m=0}^{M-1}\left|\mathcal{A}_{A_k s_k(t),s_k(t)}(\nu,\tau)\right|^2}{\frac{1}{M}\sum_{m=0}^{M-1}\left|\mathcal{A}_{\sum_{k\neq i} A_i s_i(t),s_k(t)}(\nu,\tau)\right|^2}. \tag{10}$$

The $\overline{\mathrm{SIR}}$ with varying τ and zero frequency shift as well as the $\overline{\mathrm{SIR}}$ with varying ν with zero time lag has been simulated for $K = 4$ and $K = 32$ and are shown in Fig. 5. The signals have been heavily oversampled to approximate continuous-time signals and the symbol time T_s of the Fourier basis signals has been adjusted to have an AF with comparable sensitivity. In line with our initial goal and as visible in Fig. 5, the $\overline{\mathrm{SIR}}$ as a function of time-lag and frequency-shift is considerably better for Fourier-Hermite signals than for Hermite functions. The SIRs based on the sets of Fourier-Hermite and Fourier basis signals are quite similar for $K = 4$ and for higher K the Fourier-Hermite basis are slightly more robust against a time-frequency offset than the Fourier basis. As a remark, the SIR per subcarrier reveals that for large K some Fourier-Hermite signals become more sensitive to a time-offset and others become more sensitive to a frequency-offset (which could also be concluded from Fig. 3).

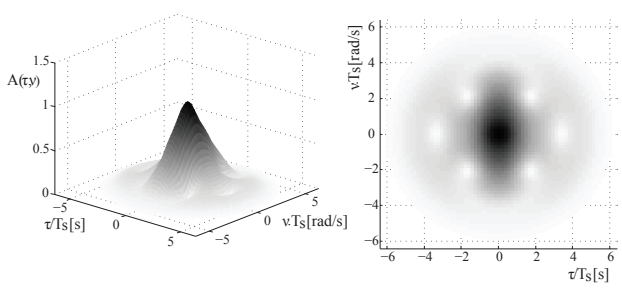

Fig. 4. Auto-ambiguity function of $s_{k=0,\mathrm{FH}}$ when $K = 4$; side-view (left) and top-view (right). The auto-ambiguity functions for $s_{k\neq 0,\mathrm{FH}}$ are equal to $s_{k=0,\mathrm{FH}}$, but rotated.

4. RELATION TO PRIOR WORK

Better time-frequency localization has been pursued by prolate spheroidal wavefunctions (PSWFs) [2], Gabor frame theory [9], wavelets and filter bank multi-carrier systems [10]. Hermite functions play to some extent a role in all these different research fields; they are a 'subset' of the PSWFs [2], they are recently analyzed as (super)frames for multi-carrier signals [9, 11] and as pulseshaping filter for filterbank multi-carrier systems [12]. As pointed out by Kozek and Molisch, Hermite functions have a nice sharp concentration of the AF proportional to the order of the Hermite function [5]. However, the sharp concentration also causes inter-carrier interference in case of a slight synchronization error, which is the primary problem addressed in this paper. Comparative analysis of the performance in (doubly) dispersive mobile radio channels of Fourier-Hermite signals with OFDM, PSWFs and wavelets is aimed for. For sending multiple sets of Fourier-Hermite signals the work in [11] can be complementary to this paper.

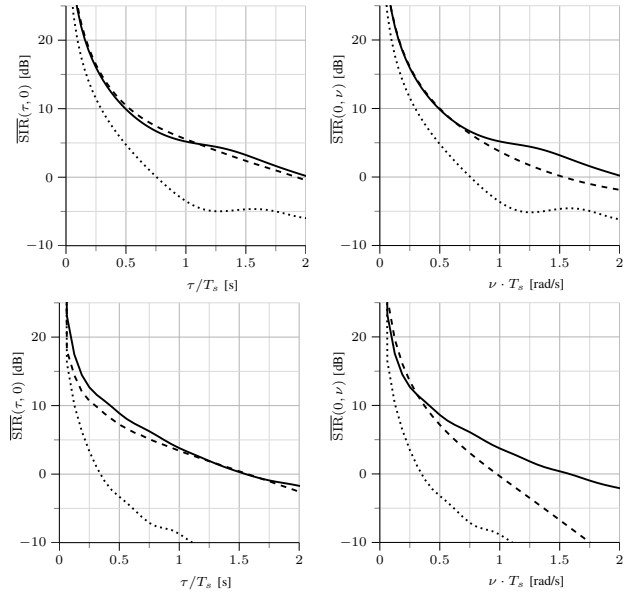

Fig. 5. The average signal-to-interference ratio (SIR) is shown for a set of Fourier (*dashed*), Hermite (*dotted*) and Fourier-Hermite signals (*solid*) as a function of either time lag τ (left) or frequency shift ν (right). The upper and lower row show the SIR plots for $K = 4$ and $K = 32$, respectively.

5. CONCLUSIONS

The proposed set of Fourier-Hermite signals are constructed by an inverse DFT operation on the Hermite basis. The obtained signals are well localized, orthogonal, have a high spectral efficiency and a robustness against synchronization errors which is similar to the robustness of Fourier basis signals. In contrast to truncated Fourier basis signals as applied in OFDM, the sidelobes of Fourier-Hermite signals are in-band rather than out-of-band. Additional research is recommended to assess the performance in various mobile radio channels and to further investigate variations on the proposed signal set. Based on discussed properties and initial results, the Fourier-Hermite signal set is a promising candidate for communications in spectrum-scarce environments and may prove useful in other contexts as well.

6. ACKNOWLEDGMENT

The presented work was supported by the Dutch TSP project. It has joint funding from the European Regional Development Fund and the Dutch provinces of Gelderland and Overijssel.

7. REFERENCES

[1] H. Mahmoud, T. Yucek, and H. Arslan, "OFDM for cognitive radio: merits and challenges," *Wireless Communications, IEEE*, vol. 16, no. 2, pp. 6–15, 2009.

[2] D. Slepian and H. O. Pollak, "Prolate spheroidal wave functions, Fourier analysis and uncertainty - part 1," *Bell System Technical Journal*, vol. 40, no. 1, pp. 43–64, 1961.

[3] L. B. Almeida, "The fractional Fourier-transform and time-frequency representations," *IEEE Trans. on Signal Processing*, vol. 42, no. 11, pp. 3084–3091, 1994.

[4] C. W. Korevaar, A. B. J. Kokkeler, P. T. de Boer, and G. J. M. Smit, "Synchronization and matched filtering in time-frequency using the sunflower spiral," *Global Communications Conference (GLOBECOM 2012)*, pp. 1–6, 2012.

[5] W. Kozek and A. F. Molisch, "On the eigenstructure of underspread WSSUS channels," *First IEEE Signal Processing Workshop on Signal Processing Advances in Wireless Communications*, pp. 325–328, 1997.

[6] H. Nikookar and M. K. Lakshmanan, "Comparison of sensitivity of OFDM and wavelet packet modulation to time synchronization error," in *Proc. PIMRC 2008*, pp. 1–6.

[7] F. Auger, P. Flandrin, P. Gonçalvès, and O. Lemoine, "Time-frequency toolbox for use with MATLAB," 1996.

[8] L. Cohen, "Time frequency-distributions - a review," *Proc. of the IEEE*, vol. 77, no. 7, pp. 941–981, 1989.

[9] K. Gröchenig and Y. Lyubarskii, "Gabor (super)frames with Hermite functions," *Mathematische Annalen*, vol. 345, pp. 267–286, 2009.

[10] B. Farhang-Boroujeny, "OFDM versus filter bank multicarrier," *Signal Processing Magazine, IEEE*, vol. 28, no. 3, pp. 92–112, may 2011.

[11] M. Hartmann, M. Gerald, and S. Dieter, "Wireless multicarrier communications via multipulse Gabor Riesz bases," *EURASIP Journal on Advances in Signal Processing*, pp. 1–15, 2006.

[12] B. Farhang-Boroujeny and C. H. Yuen, "Cosine modulated and offset QAM filter bank multicarrier techniques: A continuous-time prospect," *Eurasip Journal on Advances in Signal Processing*, pp. 1–16, 2010.